Accelerator Division

ESS AD Technical Note
ESS/AD/0036

Oscar González, Juan Luis Muñoz and Ibon Bustinduy

Preliminary Electromagnetic Design of the Re-bunching RF Cavities for the ESS MEBT

6 March 2012

Preliminary Electromagnetic Design of the Re-bunching RF Cavities for the ESS MEBT

Oscar González, Juan Luis Muñoz, Ibon Bustinduy
ogonzalez@essbilbao.org, jlmunoz@essbilbao.org, ibustinduy@essbilbao.org
ESS Bilbao

December 2011

Contents

1 Introduction and Motivation

The Medium Energy Beam Transport (MEBT) section of the ESS Linear Accelerator (linac) will be composed of several magnetic quadrupoles, re-bunching cavities, beam choppers, beam dumps and a diagnostic bench. After the beam is accelerated up to 3 MeV in the Radio Frequency Quadrupole (RFQ) cavity, the longitudinal and transversal bunches of particles are slightly broadened. The main task of the re-bunching cavities in the MEBT is to maintain the longitudinal focusing and to match the beam from the RFQ into the MEBT and from the MEBT into the Drift Tube Linac (DTL). This report summarizes the work done on the ElectroMagnetic (EM) design of the re-bunching cavities. The EM design is not independent of other design issues (tuning scheme, mechanical design, ...), so although there will be specific technical reports on these subjects, some aspects will be discussed also in this document.

2 Cavity Parameter Definition

In all RF accelerators energy is delivered to the beam from an RF electric field, which must be synchronous with the beam for a sustained energy transferred. In this section, some important parameters that characterize the energy-gain process and therefore the acceleration in RF cavities are presented.

2.1 Energy Gain on Axis of an RF Cavity

In the ESS linac, energy is transferred to a particle from the electromagnetic standing waves occurring in the RF cavities. The electric field on the axis experienced by a particle with a velocity v can be expressed as

$$E_z(r=0,z,t) = E_z(0,z)\cos\left[wt(z)+\phi\right] \tag{1}$$

where

$$t(z) = \int_0^z \frac{dz}{v(z)} \tag{2}$$

is the time the particle is at position z. We choose time $t=0$ when the particle is at the origin, which is usually defined as the geometrical center of the cavity. At $t=0$, the phase of the field relative to the crest is ϕ.

Suppose that the cavity has an axial length L. Then, the energy gain of an arbitrary particle with charge q traveling through the cavity is

$$\triangle W = \int_{-L/2}^{L/2} \vec{F}\cdot d\vec{l} = q\int_{-L/2}^{L/2} \vec{E}\cdot d\vec{l} = q\int_{-L/2}^{L/2} E_z(0,z)\cos\left[wt(z)+\phi\right]dz,$$

which using a well-known trigonometric identity can be expressed as

$$\triangle W = q\int_{-L/2}^{L/2} E_z(0,z)\left[\cos wt\cos\phi - \sin wt\sin\phi\right]dz. \tag{3}$$

Next, we can write eq. (3) in the form

$$\triangle W = qV_0T\cos\phi, \tag{4}$$

where we have introduced an axial RF voltage, defined by

$$V_0 = \int_{-L/2}^{L/2} E_z(0,z)dz, \tag{5}$$

and the transit-time factor, defined as

$$T = \frac{\int_{-L/2}^{L/2} E_z(0,z)\cos\left[wt(z)\right]dz,}{V_0} - \tan\phi\frac{\int_{-L/2}^{L/2} E_z(0,z)\sin\left[wt(z)\right]dz}{V_0}. \tag{6}$$

Equation (4) is an important result. Although it is simple in appearance, much of the physics is contained within it. This is why it deserves a carefully study of each one of its constituents:

- The relative phase ϕ indicates whether the particle arrives at the origin when the field is at a crest. The phase $\phi = 0$ if the particle arrives at the origin when the field is at the crest. It is negative if the particle arrives at the origin earlier than the crest and positive if it arrives later. Maximum energy gain occurs when $\phi = 0$.

- V_0 is the voltage gain in the cavity. V_0T is called the *effective voltage* and it is usually a design parameter. It is useful to define an average axial electric-field amplitude

$$E_0 = \frac{V_0}{L}. \tag{7}$$

  V_0 is the voltage gain that would be experienced by a particle passing through a constant DC field equal to the field in the cavity at time $t = 0$. The value of E_0, which is an average field over the length L, does not depend on the choice of L. Therefore, when a value of E_0 is quoted for a cavity, it is important to specify the corresponding length. E_0T is often called the *accelerating gradient*.

- The Transit Time Factor (T) is the ratio of energy gained in the time-varying RF field to that in a DC field of voltage $V_0\cos\phi$. Thus T is a measure of the reduction in the energy gain caused by the sinusoidal time variation of the field in the cavity. Since both ϕ and T depend on the choice of the origin, it is convenient to simplify the T expression given in (6), and remove its dependence on the phase. To do so, we must choose the origin at the electrical center of the cavity. Moreover, if $E_z(0,z)$ is an even function about the geometric center of the cavity, both the electrical center and the geometric center of the cavity coincide and T becomes

$$T = \frac{\int_{-L/2}^{L/2} E_z(0,z)\cos\left[wt(z)\right]dz,}{V_0}, \tag{8}$$

  since

$$0 = \int_{-L/2}^{L/2} E_z(0,z)\sin\left[wt(z)\right]dz$$

  applies. Therefore the expression for T in equation (8) is the average of the cosine factor weigthed by the field. In most cases, the change of particle velocity in the cavity is small compared with the initial velocity, thus equation (2) can be approximated by $t \approx z/v$, thus

$$wt \approx \frac{wz}{v} = \frac{2\pi f z}{\beta c} = \frac{2\pi z}{\beta\lambda},$$

  where $\beta = v/c$ is the normalized velocity and $\beta\lambda$ is the distance the particle travels in an RF period. The transit-time factor simplifies to the following practical form

$$T = \frac{\int_{-L/2}^{L/2} E_z(0,z)\cos\left(\frac{2\pi z}{\beta\lambda}\right)dz,}{V_0}. \tag{9}$$

2.2 Relativistic Velocity and Energy of a Particle

Consider a particle of mass m and speed v. If c is the speed of light, a normalized velocity

$$\beta = \frac{v}{c}, \tag{10}$$

a relativistic mass factor

$$\gamma = \frac{1}{\sqrt{1-\beta^2}}, \tag{11}$$

and a kinetic energy

$$W = (\gamma - 1)\, mc^2 \tag{12}$$

can be defined. It is important to point out that for nonrelativistic particles ($\beta \ll 1$):

$$\gamma = \frac{1}{\sqrt{1-\beta^2}} \approx 1 + \frac{\beta}{2}$$

and therefore equation (12) reduces to the well-know expression for the nonrelativistic kinetic energy

$$W = \frac{mv^2}{2}.$$

Equations (11) and (12) allow us to calculate the kinetic energy from the normalized velocity β of a particle.

The inverse conversions to compute β from a given kinetic energy are

$$\gamma = \frac{W + mc^2}{mc^2}, \qquad \beta = \sqrt{1 - \frac{1}{\gamma^2}}. \tag{13}$$

2.3 Figures of Merit of a Cavity for Particle Acceleration

There are several figures of merit that are commonly used to characterize accelerating cavities. Some of these depend on the power, which is dissipated because of electrical resistance in the walls of the cavities.

2.3.1 Quality Factor

The quality factor is defined as

$$Q = w\frac{(\text{average energy stored})}{(\text{energy loss/second})} = w\frac{W_m + W_e}{P} = w\frac{W_m + W_e}{P_c + P_d} \tag{14}$$

where w is the angular resonant frequency, W_m and W_e are the magnetic and electric energies

$$W_m = \frac{\mu}{4}\,\mathrm{Re}\int_V \vec{H}\cdot\vec{H}^* dv, \tag{15a}$$

$$W_e = \frac{\epsilon}{4}\,\mathrm{Re}\int_V \vec{E}\cdot\vec{E}^* dv, \tag{15b}$$

P_c is the average power loss due to the finite conductivity of the conducting walls

$$P_c = \frac{R_s}{2}\int_{walls} \vec{H}_{\tan}\cdot\vec{H}^*_{\tan} ds = \frac{R_s}{2}\int_{walls}\left(\hat{n}\times\vec{H}_{\tan}\right)\cdot\left(\hat{n}\times\vec{H}_{\tan}\right)^* ds \quad \text{or} \tag{16a}$$

$$P_c = \int \mathrm{Re}\left(\vec{S}\cdot\hat{n}\right) ds = \int \mathrm{Re}\left[\left(\frac{1}{2}\cdot\vec{E}\times\vec{H}^*\right)\cdot\hat{n}\right] ds \tag{16b}$$

where R_s is the surface resistance defined as

$$R_s = \sqrt{\frac{w\mu}{2\sigma}}, \tag{17}$$

P_d is the average power loss due to dielectric losses

$$P_d = \frac{1}{2}\,\mathrm{Re}\int_V \vec{J}\cdot\vec{E}^* dv. \tag{18}$$

and P is the total dissipated power. At resonance $W_m = W_e$, therefore only one of the two energies have to be computed.

As a conclusion, Q is a measure of the loss of a resonant cavity: lower loss implies a higher Q.

2.3.2 Shunt Impedances

The shunt impedance is defined as

$$r_s = \frac{V_0^2}{P}, \tag{19}$$

where V_0 is the axial voltage defined in (5) and P is the dissipated power calculated from equations (16) and (18). This parameter is independent of the excitation level of the cavity and measures the effectiveness of producing and axial voltage V_0 for a given dissipated power.

In an accelerating cavity we are really more interested in maximizing the particle energy gain per unit power dissipation. According to (4), the peak energy gain of a particle occurs when $\phi = 0$, and is $\triangle W = qV_0T$. Consequently, we define an effective shunt impedance of a cavity as

$$r = \left[\frac{\triangle W_{\phi=0}}{q}\right]^2 \frac{1}{P} = \frac{[V_0T]^2}{P} = r_sT^2. \tag{20}$$

This parameter in megohms measures the effectiveness per unit power loss for delivering energy to a particle.

For a given field, both V_0 and P increase linearly with L, as do both r and r_s. For long cavities we often prefer a quantity that is independent of both the field level and the cavity length. Thus, it is also convenient to introduce *shunt impedances* per unit length. The shunt impedance per unit length, Z, is simply

$$Z = \frac{r_s}{L} = \frac{V_0^2}{PL}. \tag{21}$$

Analogously, the effective shunt impedance per unit length is

$$ZT^2 = \frac{r}{L} = \frac{[V_0T]^2}{PL}. \tag{22}$$

The units for quantities (21) and (22) are usually megohms per meter. Specially for normal-conducting cavities, one of the main objectives in cavity design is to choose the geometry to maximize effective shunt impedance per unit length. This is equivalent to maximizing the energy gain in a given length for a given power loss.

Another useful parameter is the ratio

$$\frac{ZT^2}{Q},$$

also called characteristic impedance of the cavity, which exclusively depends on the cavity geometry, being independent of the surface properties that determine power losses.

2.4 RF Electric Breakdown: Kilpatrick Criterion

At sufficiently high fields, room-temperature copper cavities will suffer electric breakdown or sparking. In the 1950s, W. D. Kilpatrick [4] analyzed the data on RF breakdown, and defined the conditions that would result in breakdown-free operation. The Kilpatrick results were expressed in a convenient formula by T. J. Boyd [5] given as

$$f(\text{MHz}) = 1.64E_k^2 e^{-8.5/E_k}, \tag{23}$$

where f is the frequency in MHz, E_k is the *Kilpatrick limit* expressed in megavolts per meter. Note that for a given operating frequency, (23) must be solved implicitly to obtain the corresponding *Kilpatrick limit*. Moreover, E_k increases with increasing frequency.

The *Kilpatrick criterion* is based on experimental results that were obtained in an era before clean vacuum systems were common. Therefore, the Kilpatrick criterion is considered conservative by today´s standards. The maximum peak surface field E_s in an accelerating cavity is expressed as

$$E_s = bE_k, \tag{24}$$

where b is known as the *bravery factor*. Typical values chosen for b range from 1.0 to 2.0. Larger values of b are often chosen for pulsed accelerators with pulse lengths less than about 1 ms.

3 Re-Bunching Cavity Design

3.1 Design Criteria

When designing the cavity, some considerations must be taken into account:

- The resonant frequency of the accelerating mode of the cavity is the frequency of operation of the linac.
- A high shunt impedance per unit length ZT^2, defined as in (22), is desirable in order to reduce the power consumption and therefore to simplify the cooling system.
- Electrical discharge (sparking) must be avoided by limiting the peak surface electric field. A value for the *Kilpatrick limit* or the *bravery factor* defined in (24) must be chosen.
- The cavity has to fit inside the mechanical limits imposed by the MEBT optical design, leading to a more compact structures.

The design procedure takes the work done by C. Plostinar et al. for the ISIS-FETS re-bunching cavities [1]-[3] as starting point. In their work, two basic geometries were considered as cavity candidates: the Drift Tube Linac (DTL)-type cavity and the Coupled Cavity Linac (CCL)-type cavity. Both resemble pillbox cylindrical cavities with re-entrant noses in the near axis region. The study performed by the authors lead to several remarks:

- The DTL-type cavity is more compact that the CCL cavity design, thus allowing some of the magnetic quadrupoles to be integrated inside the drift tube.
- The shunt impedance of the CCL cavity is about 3 times higher than the DTL buncher. This is so because the dissipated power is about 3 times smaller.
- The CCL cavity is easier to engineer than the DTL one.

As a conclusion, Plostinar et al. chose the CCL cavity as their candidate for the re-bunching cavity. Therefore, this is the cavity geometry that has been investigated in ESS-Bilbao.

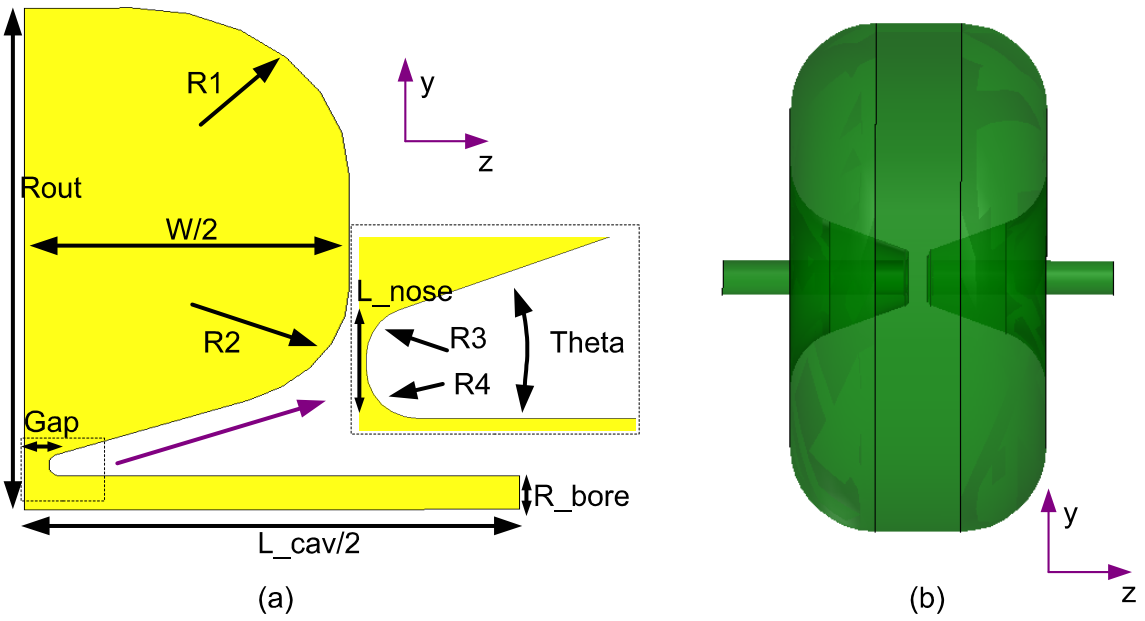

Figure 1: Re-bunching cavity designed at ESS-Bilbao. (a) Cut view of one-quarter of the cavity including the design parameters; (b) 3D vacuum model of the cavity.

3.2 Electromagnetic Model

A cut view of one-quarter of the designed cavity including its parameters is shown in Fig. 1-a. A full 3D model of the cavity (Fig. 1-b) can easily be obtained by sweeping the parametrized face 360^o around the z-axis. Finally, a mirror operation must be applied on the XY plane. Copper ($\sigma = 5.8 \times 10^7$ S/m, $\mu_r = 0.999991$) is assumed as the material for the conducting walls of the cavity.

3.3 Resonant Mode

The cavity is designed to operate in the TM_{010} mode. This mode, also called *the accelerating mode*, only has two field components: the longitudinal component of the electric field E_z and the transversal component of the magnetic field intensity H_θ. The electric field grows along the longitudinal (z) axis and its maximum value arises in the gap region, as shown in Fig. 2-a. On the other hand, the magnetic field mainly concentrates around the nose cones, thus becoming a region with high losses (Fig. 2-b). When designing the cavity, it is important to keep in mind that the accelerating mode TM_{010} is the dominant mode as long as `L_cav/2` is smaller than the cavity radius `R_out`. If this is not fulfilled, the TE_{111} mode becomes the dominant mode.

3.4 Simulation Set-Up

The re-bunching cavity has been designed and analyzed by Full-Wave electromagnetic simulators. Specifically, CST Microwave Studio (MWS), HFSS from Ansoft, COMSOL and SUPERFISH have been used. The eigenmode solver has been activated for all simulators. For CST MWS the Jacobi-Davidson method (JDM) has been chosen. According to CST documentation "the solver time for the JDM eigenmode solver increases with the number of modes to calculate. Therefore, it is usually the method of choice if only a few modes are required". For the rest of simulators, only one eigenmode solver is available.

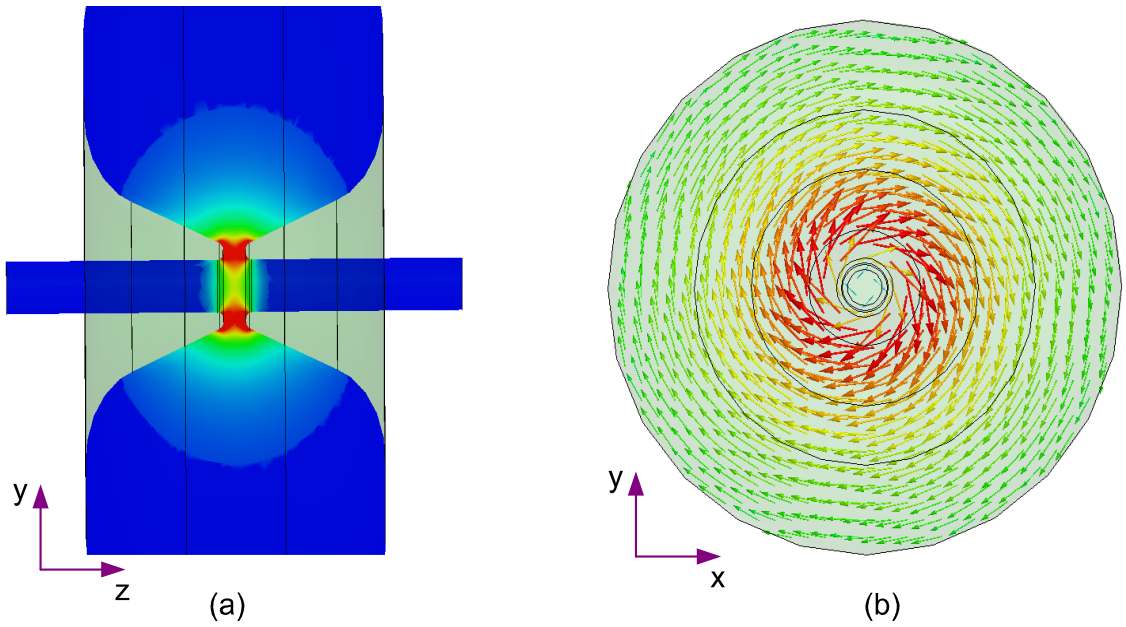

Figure 2: Field distribution of the TM_{010} for the re-bunching cavity of Fig. 1. (a) E_z electric field and (b) H_θ magnetic field. The fields are mainly concentrated on the nose cone regions.

Due to the symmetries of the TM_{010} mode, 1 Perfect Electric Wall (PEW) and 2 Perfect Magnetic Walls (PMW) can be defined in the cavity, thus only one-eighth of the 3D cavity is actually simulated. Moreover, when using COMSOL and SUPERFISH, the 2D axysimmetric option can also been activated and a simulation of the 2D geometry shown in Fig. 1-a can straight be performed. This option leads to a reduction in the computational cost of the simulations.

3.5 Cavity Specifications

The main cavity specifications have been specified by the MEBT beam dynamics design:

- A resonant frequency of 352.2 MHz (corresponding to that of the whole linac).
- An effective voltage (V_0T) of 140 kV.
- A Kilpatrick limit or bravery factor of $b = 1.4$. According to (23), $E_k = 18.45$ MV/m at 352.2 MHz, thus taking into account (24), the maximum allowed peak surface field is $E_{\mathbf{s,max}} = 25.83$ MV/m**.**
- The kinetic energy of the protons of the MEBT is $W = 3$ MeV, which according to (13) corresponds to a normalized velocity of $\beta = 0.0797320$.
- An aperture of 30 mm (`R_bore`=15 mm)
- A maximum length of 126 mm (`L_cav=W`=126 mm)

With this cavity specifications, a serial number to name the cavity has been created: *A30W126T45,* where $A30$ stands for an aperture of 30 mm, $W126$ stands for a TOTAL cavity length of 126 mm and $T45$ stands for a theta angle of 45^o. Besides these input parameters, the name of each developed prototype will be followed by the corresponding version number.

Parameter	Nominal Value, [mm]
R_bore	15
L_cav=W	126
Gap	6
L_nose	8
R_out	241
R1	30
R2	50
R3=R4	4
Theta	45

Table 1: Preliminary parameter values for the A30W126T45v0 cavity of figure 1.

Software	HFSS	CST	COMSOL	SUPERFISH
Freq, [MHz]	352.20	352.17	352.19	352.24
$\mathbf{Q_0}$	23507	23845	23514	23516
T	0.582	0.589	0.589	0.588
$\mathbf{V_0T}$**, [kV]**	140	140	140	140
P, [kW]	14.794	14.27	14.41	14.62
r, $[\mathbf{M\Omega}]$	1.32	1.37	1.36	1.33
$\mathbf{ZT^2}$**,** $[\mathbf{M\Omega/m}]$	10.51	10.87	10.79	10.59
$\mathbf{E_{s,max}}$**, [MV/m]**	30.18	28.41	26.60	25.97
Kilpatrick (b)	1.63	1.54	1.44	1.41

Table 2: Computed figures of merit for the A30W126T45v0 cavity of figure 1 and table 1.

3.6 Preliminary Results: A30W126T45_v0

Taking into account the cavity specifications mentioned above, an initial parameter sweep has been done in order to match the desired resonance frequency of the cavity. Although the resulting geometry will not be optimized from both the effective shunt impedance ZT^2 and the *Kilpatrick limit* viewpoints, it will allow us to check the accuracy of the different simulators involved. Moreover it will be our starting point to perform a parametric study. Table 1 shows the preliminary set of parameters found for the re-bunching cavity of figure 1-a. The prototype is named as *A30W126T45_v0.*

The main figures of merit computed with each of the available simulators are shown in table 2. Moreover, figure 3 shows the normalized E_z field along the axis of the cavity. Generally speaking, a good agreement among the results provided by all simulators is observed. Specifically, some aspects can be pointed out:

1. The resonance frequency of the TM_{010} is well predicted by all simulators.

2. The quality factor provided by CST is slightly higher than the one given by the other simulators. This also implies a lower dissipated power.

3. The results obtained for the shunt impedances and the transit time factor show good agreement.

4. Finally, the computed maximum peak surface field $\mathbf{E_{s,max}}$ shows the worst agreement among simulators. This computation has a strong dependence with the initial mesh settings on the surface of the cavity for each of the simulators.

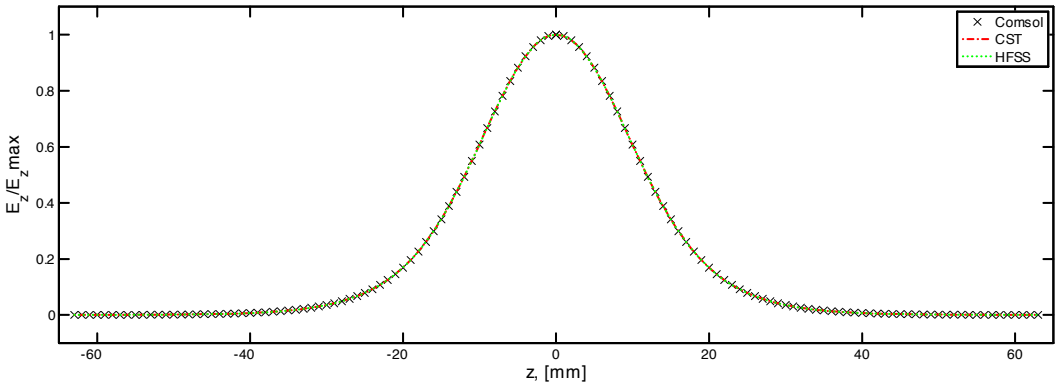

Figure 3: Normalized E_z field along the axis of the cavity *A30W126T45v0* calculated by HFSS, CST and Comsol.

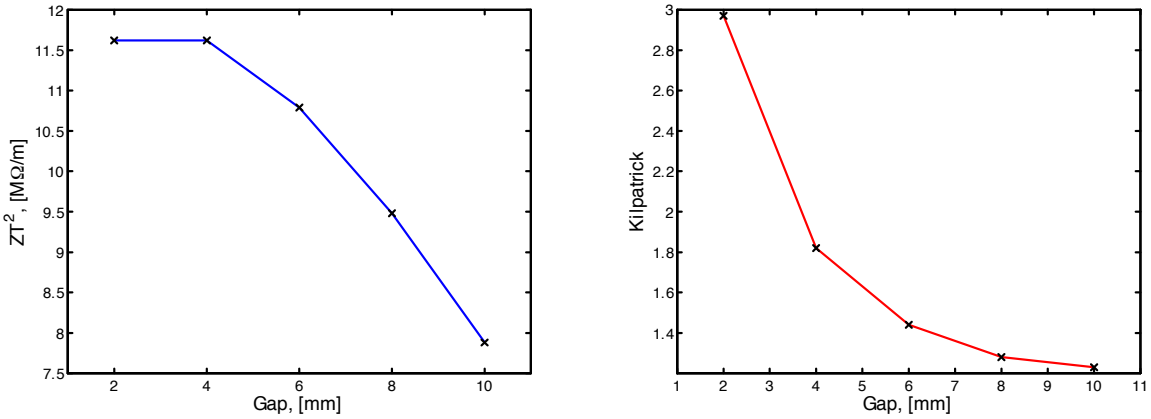

Figure 4: (a) Effective shunt impedance ZT^2 and (b) Kilpatrick factor as function of `Gap`. The values for the rest of parameters used in the simulations have been taken from table 1.

4 Parametric Analysis

In order to gain experience on how the cavity behaves, and to be able to find the optimum cavity geometry, a parametric analysis has been performed with Comsol. Starting from the nominal values given in table 1, the effect of each parameter on both the shunt impedance ZT^2 and the Kilpatrick factor has been independently studied.

4.1 Gap

As stated earlier, the nose cones concentrate a high electric field in the gap region. Thus, a right choice of the parameter `gap` is crucial. Figure 4-a shows that decreasing the `gap` has the effect of increasing ZT^2. This is so, because when the `gap` decreases, the transit time factor T increases. However, if the `gap` becomes too small, the voltage gain V_0 in the cavity is reduced thus having a negative effect on ZT^2 as it can be seen for *gap* values of less than 4 mm. In addition, as shown in 4-b, a small gap increases $E_{\mathbf{s,max}}$ which lead to unacceptable values of the Kilpatrick limit.

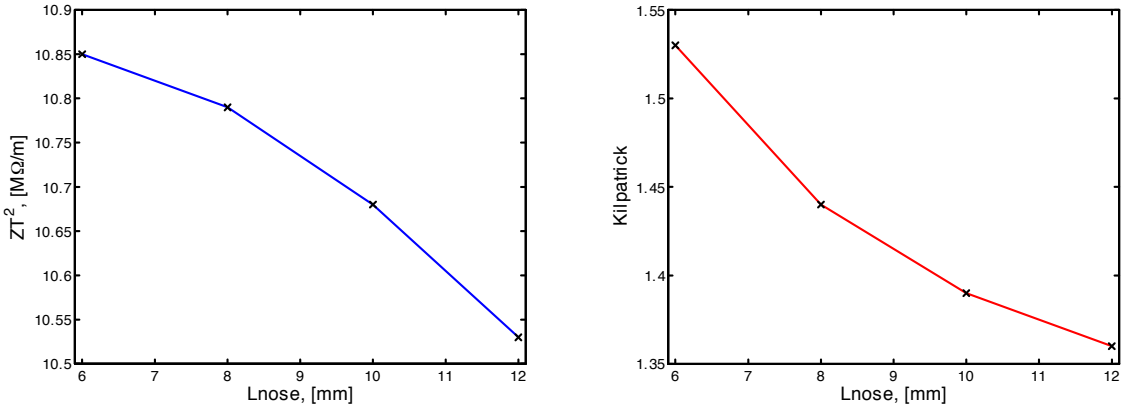

Figure 5: (a) Effective shunt impedance ZT^2 and (b) Kilpatrick factor as function of `Lnose`. The values for the rest of parameters used in the simulations have been taken from table 1.

4.2 Lnose

Since `Lnose` is a parameter also located in the nose-cone area, its behavior is quite similar to the one detected for the *gap*. However, as shown in Fig. 5, while its effect on ZT^2 is not so critical, the Kilpatrick limit is considerable reduced as the parameter increases. This could be a good choice to ensure the specified value for the Kilpatrick limit.

4.3 Cone Angle Theta

The dependence on the nose cone angle `Theta` is shown in Fig. 6. It can be seen that the highest ZT^2 correspond to the minimum value of `Theta`. However, the final value for this angle will also be chosen taking into account the space required if focusing devices are to be located on the outside part of the cavity, as proposed in [1]. Moreover, a value of `Theta` too small could result in a fragile mechanical structure as well as making the cooling of the nose cone region much more difficult.

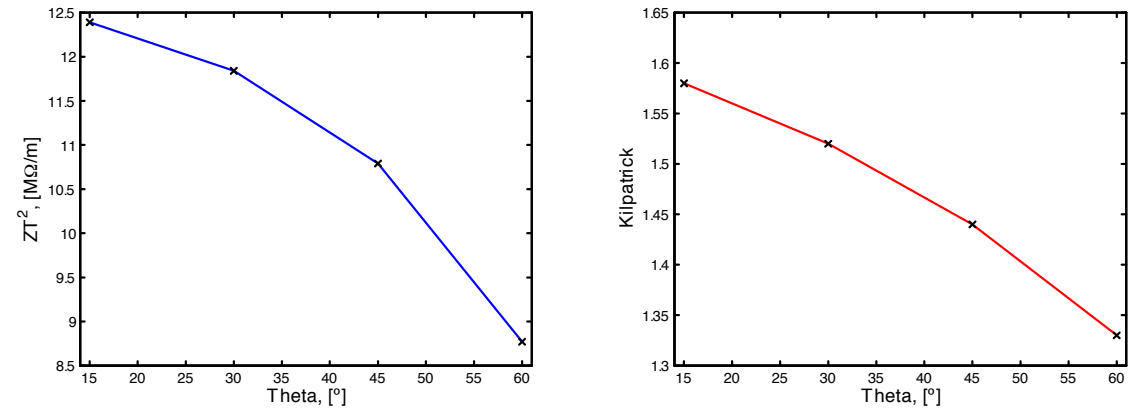

Figure 6: (a) Effective shunt impedance ZT^2 and (b) Kilpatrick factor as function of `Theta`. The values for the rest of parameters used in the simulations have been taken from table 1.

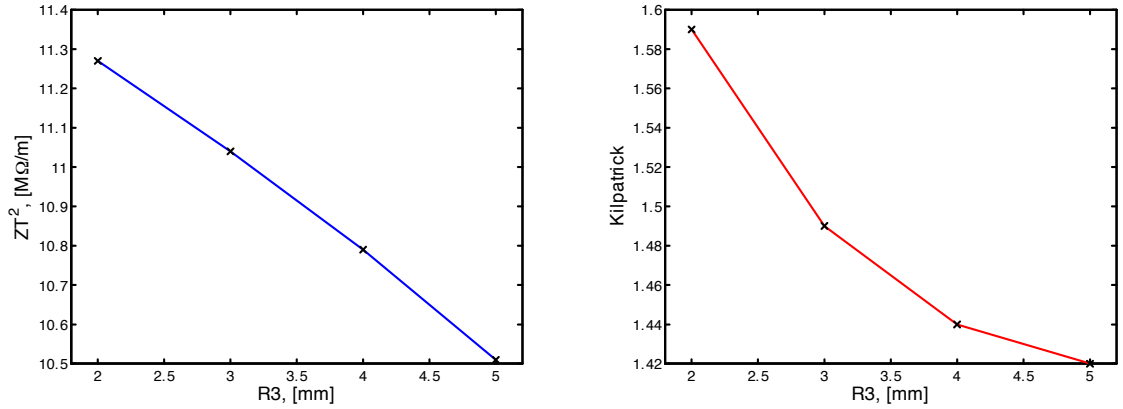

Figure 7: (a) Effective shunt impedance ZT^2 and (b) Kilpatrick factor as function of `R3`. The values for the rest of parameters used in the simulations have been taken from table 1.

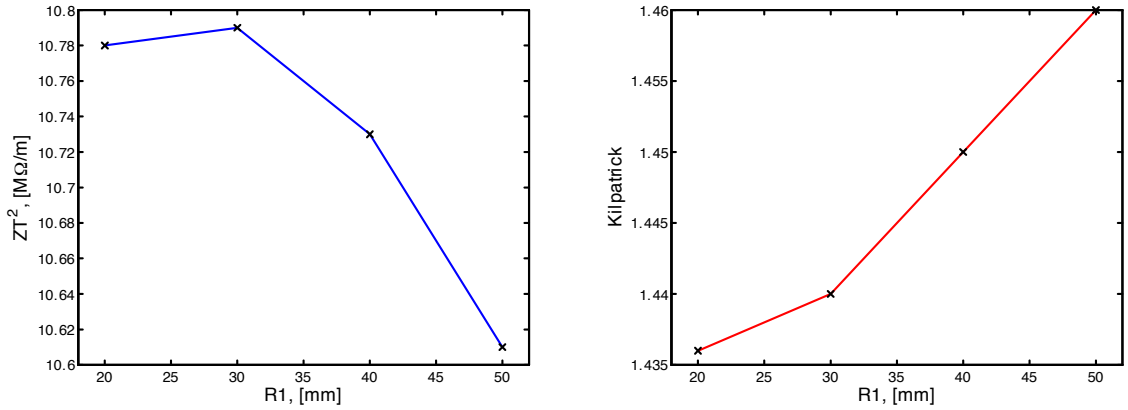

Figure 8: (a) Effective shunt impedance ZT^2 and (b) Kilpatrick factor as function of `R1`. The values for the rest of parameters used in the simulations have been taken from table 1.

4.4 Inner Radius R3 and R4

Since these parameters are related to the shape of the nose cones, their effect on the cavity figures of merit also deserves a special attention. As depicted in Fig. 7, when `R3` increases, both the Kilpatrick factor and $\mathbf{ZT}^2$ become smaller. Making `R3` greater could be a good choice.

4.5 Outer Radius R1 and R2

Contrary to what happens with all previous parameters, the outer radius `R1` and `R2` are located far from the nose cones, thus their effects on both $\mathbf{ZT}^2$ and the Kilpatrick factor should be less critical. As expected, figures 8 and 9 shows how `R1` and `R2` have little effect on both $\mathbf{ZT}^2$ and the Kilpatrick factor. As conclusion, since the overall effect in the figures of merit of the cavity is marginal, these parameters are good candidates to perform a fine tune of the cavity to the operating frequency once the optimized values for the rest of the parameters are found.

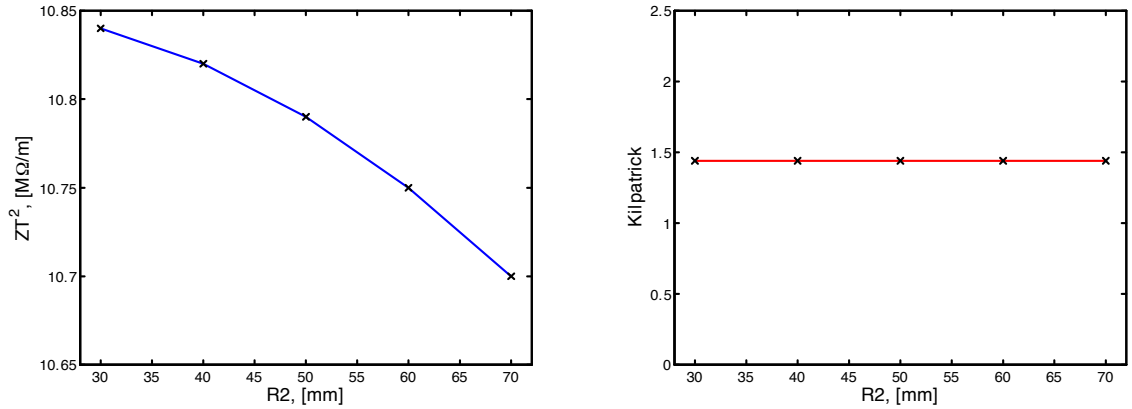

Figure 9: (a) Effective shunt impedance ZT^2 and (b) Kilpatrick factor as function of `R2`. The values for the rest of parameters used in the simulations have been taken from table 1.

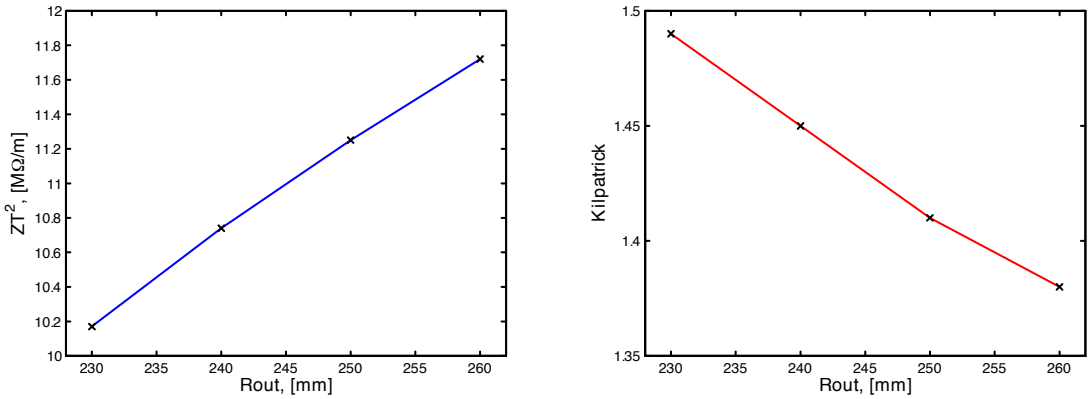

Figure 10: (a) Effective shunt impedance ZT^2 and (b) Kilpatrick factor as function of `Rout`. The values for the rest of parameters used in the simulations have been taken from table 1.

4.6 Cavity Radius Rout

Figure 10 shows that $\mathbf{ZT}^2$ monotonously increases with increasing *Rout*. However, for the Kilpatrick limit, the opposite effect is observed.

4.7 Length of the Cavity: Lcav and W

Although this parameter is given by the MEBT beam dynamics design and it should remain fixed, it is important to check how it behaves. Figure 11 shows that the longer the cavity is, $\mathbf{ZT}^2$ considerable increases while the Kilpatrick factor decreases. As a conclusion, it would be interesting to consider longer cavities provided that this is allowed by the optical design of the MEBT.

From our parametric study, the following conclusions can be pointed out:

1. For the parameters close to the nose cones, the optimum value for `Gap` will lie somewhere between 4 mm and 8 mm. The optimum value for `Lnose` will be located between 7 mm and 12 mm. Finally, for `R3` this optimum value will be located between 3 mm and 5.5 mm.

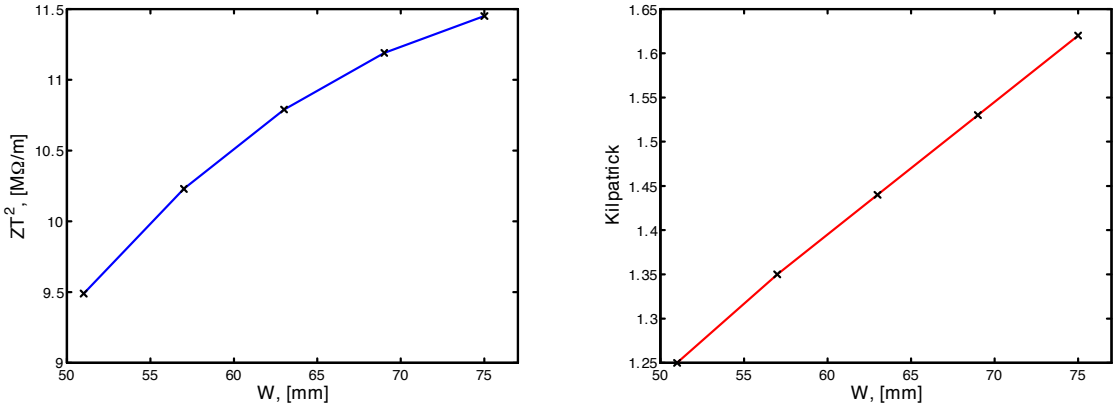

Figure 11: (a) Effective shunt impedance ZT^2 and (b) Kilpatrick factor as function of `W`. The values for the rest of parameters used in the simulations have been taken from table 1.

Parameter	**ESS Optimized, [mm]**	**CERN B30, [mm]**	**FETS, [mm]**
`R_bore`	15	15	15
`L_cav=W`	126	126	150
`Gap`	6.1	7	7
`L_nose`	7.2	8	7
`R_out`	242.5	246	303
`R1`	20	32	72
`R2`	29	60	20
`R3=R4`	3.2	5	4
`Theta`	45	45	25

Table 3: Optimized parameter values for the A30W126T45v1 ESS re-bunching cavity of figure 1. Parameters for CERN and FETS re-bunching cavities are also presented.

2. The outer radius `R1` and `R2` could be used, if needed, to perform the fine tune of the resonant frequency of the cavity.

3. The effect of `Rout` on the cavity allows us to choose the radius as big as possible, while keeping the right resonant frequency.

4. Finally, regarding the input parameters defined by the MEBT optical design, the optimum design would involved, if possible, a longer cavity and a cone angle as close as possible to 0^o.

5 Optimization Procedure: *A30W126T45_v1*

After the above parametric analysis is performed, the goal now to find the optimum geometry that will maximize the effective shunt impedance $\mathbf{ZT^2}$ while keeping the Kilpatrick limit $b \leq 1.4$. The optimization procedure has been carried out as following:

1. Besides the parameters already fixed due to cavity specifications (`R_bore`=15 mm, `L_cav=W`=63 mm), the conservative value of `Theta`= 45^o has also been fixed.

2. The CST *interpolated quasi-newton* optimizer has been activated. The parameters `Gap, L_nose, R3` and `Rout` have been optimized. A dynamic range of variation for

Model	ESS	CERN B30	FETS
Freq, [MHz]	352.20	357.22	315.86
$\mathbf{Q_0}$	23477	24129	27222
T	0.593	0.56	0.636
$\mathbf{V_0T}$**, [kV]**	140	140	160
P, [kW]	14.02	15.38	11.82
r, [MΩ]	1.4	1.27	2.35
$\mathbf{ZT^2}$**, [MΩ/m]**	11.1	10.11	15.67
$\mathbf{E_{s,max}}$**, [MV/m]**	27.2	24.25	27.56
Kilpatrick (b)	1.47	1.3	1.49

Table 4: Computed figures of merit for the optimized A30W126T45v1 cavity of figure 1 with the parameters of table 3. Results for the CERN and FETS cavities are also presented.

each of the parameters during the optimization process has been specified. This range is set according to the results obtained in the parametric analysis. Therefore, `Gap` is within [4−8] mm, `Lnose` within [7−12], `R3` within [3−5.5] and Rout between [240−250] mm. The optimizer goal is set to maximize ZT^2 while keeping the Kilpatrick limit under<1.4 and the resonant frequency $freq = 352.2$ MHz.

3. Later, $R1$ and $R2$ will be used, if needed, to perform a fine tuning of the resulting cavity. In this way, the final geometry of the cavity is defined.

4. Finally, a simulation with the final cavity geometry is performed and the figures of merit computed.

After many simulations, a set of parameters for an optimized cavity are depicted in table 3. This cavity is named *A30W126T45_ v1*. For comparison purposes, the dimensions of the rebunching cavities designed at CERN [6] and FETS (ISIS) [7] are also included. Finally, table 4 summarizes the main characteristics of the optimized cavity. Moreover the results obtained for CERN and FETS cavities are also shown. The 3 simulation results in table 4 have been obtained by using COMSOL.

A comparison between the original prototype (*A30W126T45_ v0*) and the optimized one (*A30W126T45_ v1*) leads to the following conclusions:

1. The Kilpatrick limit in the optimized cavity is smaller than the specified limit of 1.4.

2. The shunt impedance $\mathbf{ZT^2}$ is now optimized by increasing the time transit factor T and reducing the dissipated power P.

Moreover, when comparing the optimized cavity *A30W126T45_ v1* with both the *CERN B30* and the *FETS* cavity:

1. The FETS cavity is longer, bigger and has a smaller nose cone angle than the other 2 cavities. Therefore, according to figures (6), (10) and (11), this is why $\mathbf{ZT^2}$ is greater and the dissipated power P much smaller.

2. The results obtained for both *A30W126T45_ v1 ESS* and *CERN B30* cavities are quite similar. However, the ESS design show a bigger shunt impedance and a lower dissipated power while fulfilling the specification value given for the Kilpatrick limit.

6 Manufacturing Considerations

The cavity has been optimized in order to resonate at a frequency of 352.2 MHz, the operating frequency of the linac. As it will be described in a later report, the introduction in the cavity of a plunger tuner in a region of high magnetic field, will always increase the resonant frequency, so if tuners are incorporated to the design the resulting frequency of the cavity will be higher than the initial one.

Taking this into account, a brief description of the proposed mechanical fabrication process for the cavity is described here. The cavity mechanical design comprises two main pieces: one includes the cavity barrel and one cover, while the other piece includes only one cover. The procedure is iterative. After the design has been done at the right frequency (352.2 MHz), a modified design with a greater *gap* length is manufactured, thus leading to a higher resonant frequency (about 358 MHz). This model is fabricated with all the ports opened and the tuners (one fixed and one movable) in the right positions. The assembled cavity is then measured to verify the design and to check the resonant frequency. Afterwards, the cover piece edge is machined, so when the full cavity is assembled the *gap* length would be smaller (resulting in lower resonant frequency). This process continues until the desired frequency is obtained. The movable tuner range must be enough to deal with the frequency shift due to the thermal expansion of the cavity, which mainly appears on the nose cones of the *gap* area. Therefore, during operation, the cavity geometry will be very similar to the one obtained by optimizing the geometry at 352.2 MHz. Finally, for our optimized cavity, a resonant frequency of 358 MHZ will be achieved by letting a gap length of 6.8 mm.

7 Conclusions and Future Work

In this work, an electromagnetic design, a parametric analysis and an optimization of a re-bunching cavity have been presented. To this end, several full-wave electromagnetic simulators have been used. Generally speaking, a good agreement among simulators is achieved. The performance of the optimized cavity is promising in terms of the shunt impedance $\mathbf{ZT}^2$ and the Kilpatrick limit. However, much work remains to be done in the near future:

1. Once the input specifications are fully established, a re-optimization of the cavity must be performed.

2. With this optimized geometry, the power distribution in the surface of the cavity will be used as the input parameter to perform the thermal and mechanical analysis of the cavity.

3. Moreover, taking into account both the required energy and the dissipated power in the cavity, an study on the power needed for the cavity as long as the topology of the power coupler that will inject the power into the cavity will be performed.

4. Finally, a study on the tuning system required for the cavity in order to correct the frequency shift due to both the thermal expansion of the cavity and the manufacturing tolerances must be tackled.

References

[1] C. Plostinar, M. Clarke-Gayther, "Re-bunching RF cavities and hybrid quadrupoles for the RAL FETS", *EPAC 2006*, pp. 306-308 , Edinburgh, Scotland.

[2] C. Plostinar, M. Clarke-Gayther, C. Thomas, "Design progress of the re-bunching RF cavites and hybrid quadrupoles for the RAL FETS", *Internal Report.*

[3] C. Plostinar, "MEBT design for the RAL Front End Test Stand", *MOPD59, IPAC 2010*, Kyoto, Japan, 2010

[4] W. D.Kilpatrick, *Rev. Sci. Instr.* 28, 824 (1957).

[5] T. J. Jr. Boyd, *Kilpatrick´s Criterion*, Los Alamos Group AT-1 report AT-1:82-28, February 12, 1982.

[6] "CERN Re-bunching plane", Private Communication.

[7] M. Larrañaga, R. Enparantza, C. Plostinar, "Design Optimization Of The Re-Bunching Cavities For The Front End Test Stand At Ral", *MOP080, LINAC2010*, Tsukuba, Japan, 2010.